Investigation of the Effect of Chemical Treatment on the Properties of Colombian Banana and Coir Fibers and Their Adhesion Behavior on Polylactic Acid and Unsaturated Polyester Matrices

Ismael Barrera-Fajardo, Oswaldo Rivero-Romero *[ID] and Jimy Unfried-Silgado [ID]

Research Group ICT, Mechanical Engineering Department, University of Cordoba, Monteria 230002, Cordoba, Colombia; ibarrerafajardo@correo.unicordoba.edu.co (I.B.-F.); jimyunfried@correo.unicordoba.edu.co (J.U.-S.)
* Correspondence: oriveroromero@correo.unicordoba.edu.co

Abstract: In this work, the adhesion behavior of chemically treated banana and coir Colombian fibers embedded in polylactic acid (PLA) and unsaturated polyester resin (UPR) matrices was investigated. Both types of fibers were treated with a 5 wt.% sodium hydroxide solution for one hour. The properties of treated and untreated fibers were determined by scanning electron microscopy (SEM), Fourier transform infrared spectroscopy (FTIR), thermogravimetric analysis (TGA), and tensile tests. To evaluate the adhesion behavior of the fibers in PLA and UPR matrices, pull-out tests were performed, and the percentage of broken fibers was determined. The results showed that alkaline treatment improved the fibers' physicochemical, mechanical, and thermal properties. In addition, the alkaline treatment was able to improve the adhesion behavior of coir and banana fibers to PLA and UPR matrices. The banana fibers showed a percentage of broken fibers of 100%, while the coir fibers showed a slight increase in IFSS value. This behavior is attributed to the improvement in surface roughness due to the removal of non-cellulosic composites and impurities.

Keywords: lignocellulose fibers; polymer matrix; alkali treatment; adhesion behavior; pull-out test; mechanical properties

1. Introduction

In recent years, lignocellulosic fibers have attracted great interest as a potential reinforcement material to produce polymer matrix composites due to their biodegradability, availability from renewable sources, cost, recyclability, lightweight nature, and exceptional mechanical properties, which make them viable alternatives to synthetic fibers such as carbon and glass fibers [1–3]. The fibers of the pseudo-stem of banana and the mesocarp of coconut are extracted from agro-industrial waste [4,5]. Therefore, their applicability at the industrial level is of great interest for solving waste management problems in agro-industry [6]. The integration of lignocellulosic fibers into the polymer matrix is one of the difficulties in the production of composites since the compatibility of the fibers is low due to their hydrophilic character and high pectin and wax contents on the surface. As a result, hydroxyl groups and hygroscopic organic matrices cannot interact [7]. It has been found that a weak fiber–matrix interface can lead to significant degradation of the mechanical and thermal properties of composites [8]. Therefore, various chemical treatments have been used to improve the physicochemical, mechanical, and thermal properties of the fibers [7,9]. This can result in good fiber–matrix interaction due to the presence of fewer OH functional groups on the surface of the lignocellulosic fibers and increased roughness to facilitate mechanical interlocking [9,10]. One of the most common chemical treatments for natural fibers is alkaline treatment, also known as mercerization [11]. It promotes the change in

the lignocellulosic structure of the fiber and removes non-cellulosic materials from its surface [12]. This modification could improve the adhesion of the fiber–matrix interface [13,14]. Therefore, the study of interfacial behavior is important to understand how chemically treated lignocellulosic fibers interact with polymeric matrices to produce composites [15,16]. The literature indicates that alkaline treatment affects the physicochemical and mechanical properties of coir and banana fibers, which improves their compatibility with thermoplastic and thermoset matrices and increases their potential as reinforcing materials [9,17,18].

The mechanical performance of composites is highly influenced by the fiber–matrix interface [7,14]. A weak adhesive interface decreases stress transmission between the fiber and the matrix, which can decrease the mechanical strength and stiffness of the materials. On the other hand, a strong interface generally allows good stress transmission, without disturbance, and high mechanical properties are obtained [8,19]. The interfacial strength between the composites can be investigated using pull-out tests [20]. In this test, a single fiber partially embedded in a matrix is pulled out. The maximum pull-out force and the embedded fiber length are used to determine the interfacial shear strength (IFSS) [14,21]. IFSS is calculated according to Equation (1) [7].

$$\text{IFSS (MPa)} = \frac{F_{max}}{n \cdot \pi \cdot D \cdot L}, \tag{1}$$

where F_{max} is the maximum pull-out force in N; n is the number of embedded fibers in the matrix (for a single fiber, this value is 1); D is the diameter of embedded fiber in mm; L is the length of the embedded fiber in mm [7]. The pull-out test is often performed to evaluate the interactions between the fiber and the matrix at the interface [22]. This is important in practice because most cases of fiber–matrix interface debonding occur a long time after initial use due to low cyclic loads [23]. On the other hand, the chemical treatment of lignocellulosic fibers such as coir and banana fibers embedded in a polymer matrix has a favorable effect on IFSS. Merlini et al. [24] studied the effects of chemical treatment with 10 wt.% NaOH solution on the interface between banana fibers and polyurethane matrix. The treated banana fibers showed higher tensile strength and IFSS compared to the untreated fibers, indicating a strong interaction between the treated fibers and the polyurethane matrix. Similar behavior was found by Nam et al. [25] when studying mercerized coir fibers embedded in a polybutylene succinate (PBS) matrix. Mercerization of the coir fibers increased the IFSS and wettability of the fibers by the PBS resin, which improved the mechanical properties of the composite material produced. However, few works in the available literature attempt to determine the effect of the alkaline treatment of coir and banana fibers and its influence on interfacial adhesion in polylactic acid (PLA) and unsaturated polyester resin (UPR) matrices. The latter can provide information on the performance of the fiber–matrix interface in these types of materials, as they have high potential as reinforcing materials for the fabrication of composites via 3D printing or resin transfer molding (RTM) processes [26,27].

Therefore, this work aims to study the effects of alkaline treatment on the physicochemical, mechanical, and thermal properties of banana and coir fibers and their adhesion behavior when embedded in PLA and UPR matrices. The treated and untreated fibers were characterized by scanning electron microscopy (SEM), Fourier transform infrared spectroscopy (FTIR), thermogravimetric analysis (TGA), and tensile tests. The adhesion behavior of banana and coir fibers treated with NaOH solution and untreated fibers embedded in PLA and UPR matrices was evaluated using pull-out tests.

2. Materials and Methods

2.1. Materials

Banana fibers (BF) used in this work were obtained from the pseudo-stem of a plant of the variety "Hartón" from crops in the municipality of Cerete, Cordoba, Colombia (12 MASL) at the coordinates 8°51′33″ N, 75°49′43″ W. Coir fibers (CF) were extracted from the mesocarp of a coconut of a palm tree of the variety "Cocotero gigante" from crops in

the municipality of Puerto Escondido, Cordoba, Colombia (30 MASL) at the coordinates 9°01′09″ N 76°15′41″ W. Figure 1 shows the geographical location of the banana and coconut crops at Córdoba, Colombia. Both waste materials were submerged in clean water and manually treated to extract fibers. Then, banana and coir fibers were dried at a controlled temperature of 40 and 90 °C for a period of 4 and 2 h, respectively, to obtain fibers with a moisture content of about 14% [28,29]. Bromatological analysis was performed on the dried fibers. Mass percentages of dry matter, ashes, acid detergent fiber (ADF), neutral detergent fiber (NDF), and cellulose were determined according to standard methods proposed by the Association of Analytical Communities (AOAC) International [30]. The chemical composition of the fibers measured using bromatological tests is summarized in Table 1. A commercial polylactic acid (PLA) filament for 3D printing with a diameter of Ø1.75 mm was used as the thermoplastic matrix, while an unsaturated polyester resin (UPR) (Cristalan 12 1969 RTM from Andercol, Colombia) was used as the thermoset matrix.
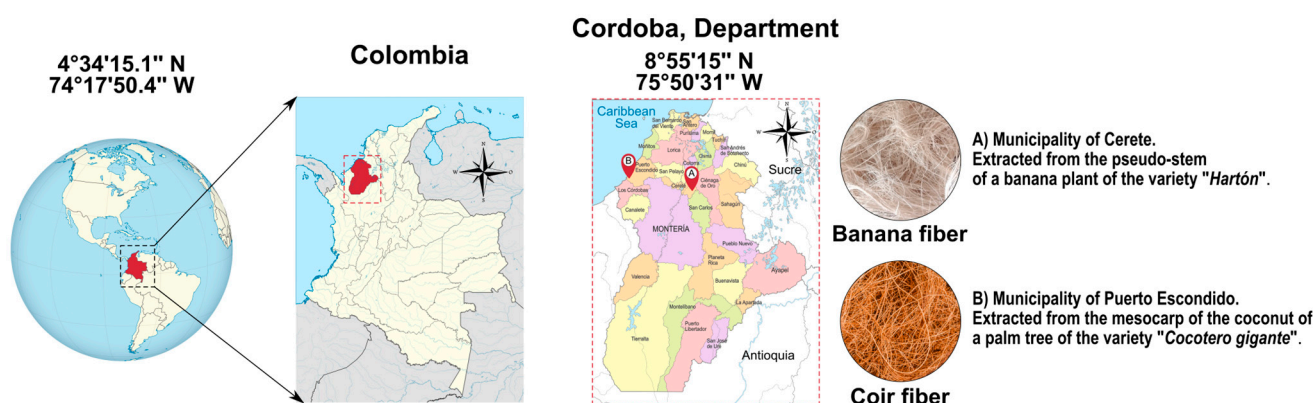
Figure 1. Geographical location of banana and coconut crops in Cordoba, Colombia [31].

Table 1. Chemical composition of fibers [28,29].

Material	Cellulose (%)	Hemicellulose (%)	Lignin (%)	Other Substances (%)
Banana fiber	41.17	11.51	13.61	33.71
Coir fiber	34.75	5.27	34.01	25.97

2.2. Alkali Treatment of Fibers

The banana and coir fibers were immersed in a 5 wt.% aqueous NaOH solution at room temperature for 1 h with periodic agitation. After that, the mercerized fibers were washed several times with acetic acid (50% *v/v*) and distilled water to remove traces of NaOH. Finally, the treated banana and coir fibers were dried in a controlled atmosphere using two temperatures, 40 and 90 °C, respectively, for 2 h.

2.3. Characterization of Fibers

2.3.1. Measurements of Mechanical Properties

Banana and coir single fibers were tensile tested according to the ASTM C1557-20 standard test [32]. The tensile tests were performed on a Shimadzu® universal testing machine, model Autograph AG-X, with a load cell of 500 N and a crosshead speed of 2 mm/min. The treated and untreated fibers were carefully fixed on a mounting tab with a calibrated length of 50 mm. The tensile properties of the fibers, i.e., tensile strength, Young's modulus, and elongation at break were measured. The tests were performed in a controlled environment with a temperature and relative humidity of 25.2 °C and 50.5%, respectively. The average diameter of the fibers was measured by optical image microscopy. A fully circular fiber cross-section was assumed, and the average value of ten transverse dimensions measured along the fiber length was determined for each sample [33,34]. A total of 80 samples of banana and coir fibers with and without alkali treatment were tensile

tested. Analysis of variance (ANOVA) was used to study the effect of fiber type and surface treatment on the mechanical properties of the fibers studied, using a significance level of 0.05.

2.3.2. Fourier Transform Infrared Spectroscopy

Treated and untreated fibers were analyzed by Fourier transform infrared spectroscopy (FTIR) on a Shimadzu IRTracer-100 spectrometer with an attenuated total reflectance (ATR) accessory detector. Spectra were obtained in a wavenumber range of 4000–500 cm^{-1} with a resolution of 1 cm^{-1}. Peaks were analyzed for comparison with open-access databases.

2.3.3. Scanning Electron Microscopy

A JEOL$^{®}$ model JSM-7100F scanning electron microscope (SEM) was used to investigate the surface morphology and cross-section before and after the mechanical tests of treated and untreated banana and coir fibers at an accelerating voltage between 5 and 10 kV. The samples were fixed to brass mount holders with carbon tape and ion sputtering coated with gold to ensure the conductivity of the organic material when exposed to the electron beam.

2.3.4. Thermogravimetric Analysis

Thermogravimetric analysis of treated and untreated fibers was performed using a TGA550 thermogravimetric analyzer (T.A. Instruments$^{®}$, New Castle, DE, USA) under a nitrogen atmosphere at a flow rate of 100 mL/min. Samples of approximately 5 mg were heated from 25 to 940 °C at a heating rate of 15 °C/min. The weight loss and derivative curve (DTG) as a function of temperature were determined and evaluated.

2.4. Fiber–Matrix Adhesion Analysis

2.4.1. Preparation of Specimen Pull-Out Test

For the evaluation of IFSS, specimens were prepared for the pull-out test with three experimental parameters, i.e., fiber type, matrix type, and surface treatment. The nomenclatures of the prepared specimens are listed in Table 2. To fabricate the specimens with a UPR matrix, square molds (14 × 14 × 5 mm) with a rectangular cavity of 10 × 10 mm and a depth of 4.0 mm were prepared using the 3D printing method. With this geometry, an embedded length (L) of about 4 mm was achieved after resin curing [35]. Single fibers were fixed and centered in the mound cavity while a mixture of UPR and 8% *v/v* peroxide Mek catalyst was poured. The samples were fully cured for 1 h at room temperature. The material used for mound printing was PET-G (polyethylene terephthalate glycol) with a commercial diameter of Ø1.75 mm, a printing temperature of 235 °C, a bed temperature of 80 °C, a layer height of 0.2 mm, and an extrusion width of 0.4 mm. Figure 2a,b show a sketch of the setup performed and the final specimen, respectively, for the pull-out specimens mounted on UPR. On the other hand, the PLA matrix samples were directly fabricated by 3D printing using an FFF 3D printer. Layers of molten PLA were deposited on the build platform up to a certain height, then, extrusion was stopped, and the single fiber was placed on the top layer of PLA volume I by fixing its two free ends to keep them straight and aligned, protruding from the printed volume. Finally, melt layers were applied to coat the fiber with PLA volume II. A PLA matrix sample of 3.5 × 10 × 10 mm was fabricated. The PLA samples were removed from the building platform after cooling. Figure 2c,d show a sketch of the setup performed and the final shape of the PLA matrix samples. In this geometry, an embedded length (L) of about 3.5 mm was achieved by cutting off one of the free ends of the fiber [34]. The print path planning was performed using the Full Control Designer G-code$^{®}$ software original version [36]. The printing parameters were set to a printing temperature of 200 °C, a bed temperature of 60 °C, a layer height of 1 mm, and an extrusion width of 2.4 mm.

Table 2. Nomenclature specimens for the pull-out test.

Fiber Type	Surface Treatment	Matrix Type	Nomenclature
Banana	Treated	UPR	BF/UPR/T
		PLA	BF/PLA/T
	Untreated	UPR	BF/UPR/U
		PLA	BF/PLA/U
Coir	Treated	UPR	CF/UPR/T
		PLA	CF/PLA/T
	Untreated	UPR	CF/UPR/U
		PLA	CF/PLA/U
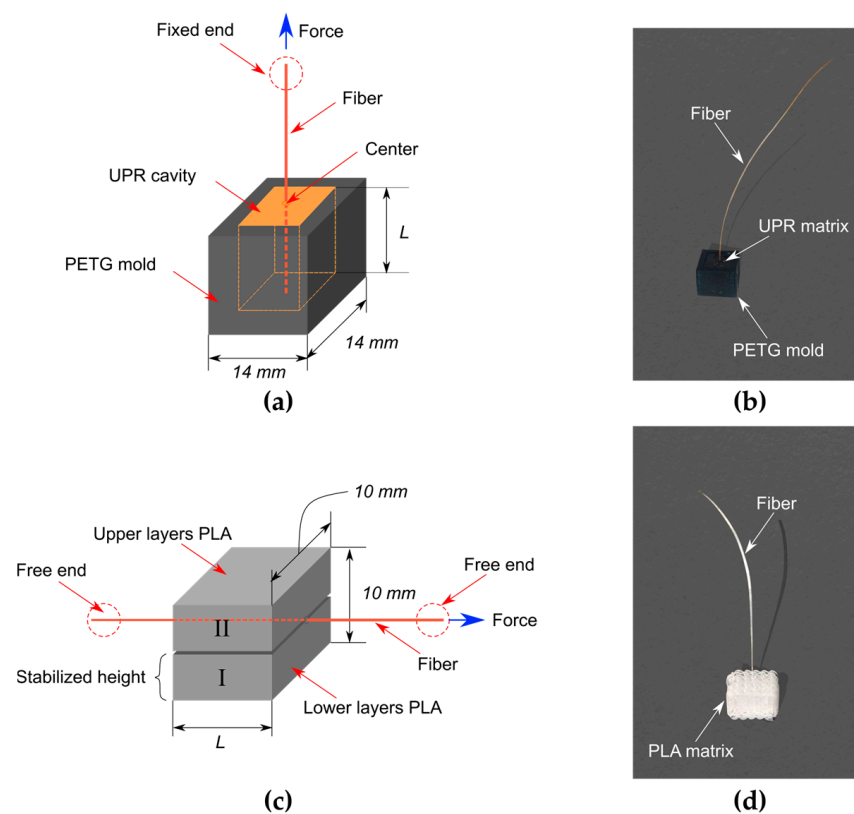
Figure 2. (**a**,**b**) UPR specimen mounting and (**c**,**d**) PLA specimen mounting.

2.4.2. Pull-Out Test

The free ends of the fibers in the specimens were carefully fixed on a mounting tap to obtain a calibrated length of 30 mm. A Shimadzu® EZ-Test machine with a load cell of 100 N was used to perform the pull-out tests, and a crosshead speed of 5 mm/min was set [37]. The specimens were clamped with the fixed lower crosshead, and the fiber was pulled out with the movable upper crosshead. The IFSS value was determined using the recorded maximum force according to Equation (1). The fiber diameter was determined by optical microscopy. A total of 42 specimens were tested. The calculations for the IFSS value were performed on specimens where the fiber could be pulled out without breakage.

3. Results and Discussions

3.1. Analysis of Mechanical Properties

The results for the tensile properties of both untreated and treated banana and coir fibers are shown in Figure 3. The average values of tensile strength, Young's modulus, and elongation at break increase slightly for the treated fibers. The mean values of both tensile

strength and Young's modulus of BF/U were 206.9 ± 80.9 MPa and 12.06 ± 4.19 GPa, respectively, while those of CF/U were 88.4 ± 34.6 MPa and 1.74 ± 0.63 GPa, respectively (see Figure 3a). However, the mean elongation at break for BF/U, with a value of 0.02 ± 0.0026, was less than that of CF/U, which had a mean value of 0.25 ± 0.0071 (Figure 3b). The abovementioned may be attributed to the fact that coir fibers tend to exhibit ductile behavior, while banana fibers exhibit brittle behavior due to the difference in cellulose content and microfibril angle (MFA) [38–40]. On the other hand, the data for BF/T and CF/T exhibited higher variability, as indicated by a higher standard deviation. This suggests that there may be no significant statistical difference in the mechanical properties between the treated and untreated banana and coir fibers.
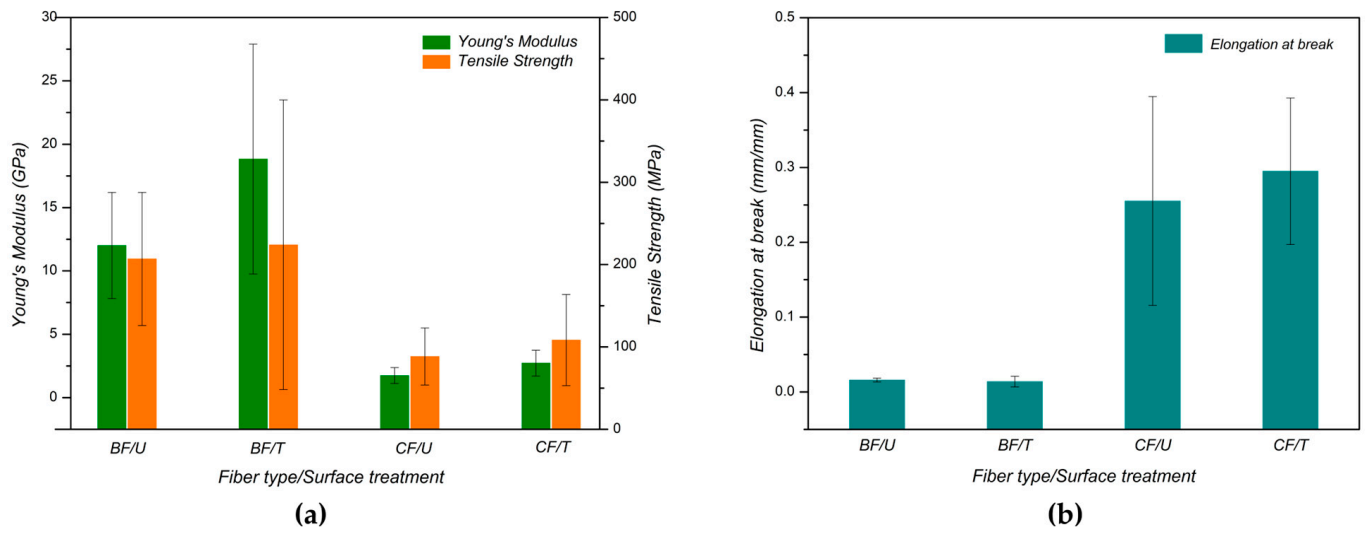

Figure 3. (**a**) Young's modulus and tensile strength, and (**b**) elongation at break of fibers under different conditions. BF: banana fiber, CF: coir fiber, T: treated condition, and U: untreated condition.

The ANOVA analyses of mechanical properties are shown in Table 3. The results indicate that only the surface treatment factor had a significant effect on the Young's modulus of coir and banana fibers. The abovementioned may be attributed to the changes in their structures due to removing the non-cellulosic components during the alkaline treatment [12]. On the other hand, it can be observed that surface treatment on fibers did not significantly affect either tensile strength or elongation at break. This can be attributed to the following two factors: First, errors in the calculation of mechanical properties since a fully circular fiber cross-section was assumed. This assumption can be considered a source of error in the measurement of the tensile properties of both treated and untreated fibers [41]. Second, the presence of micro-compressive defects or dislocations along the banana and coir fibers [42], as indicated by arrows in Figure 4. These defects have been found on the surface of natural fibers extracted by decortication or separated by hand and may affect the tensile properties of the fibers [43].

Table 3. Summary of ANOVA analysis of mechanical properties.

| Mechanical Properties	Factor Variable	DF	Adj SS	Adj Ms	F-Value	*p*-Value
Tensile Strength	Fiber type	1	165,460	165,460	14.57	0.0004 *
	Surface treatment	1	21,414.1	21,414.1	1.89	0.1761
Young's modulus	Fiber type	1	2062.62	2062.62	82.48	0.0000 *
	Surface treatment	1	269.132	269.132	10.76	0.0019 *
Elongation at break	Fiber type	1	0.8736	0.8736	110.89	0.0000 *
	Surface treatment	1	0.0037	0.0037	0.47	0.4951

* *p*-value < 0.05 = significant difference.
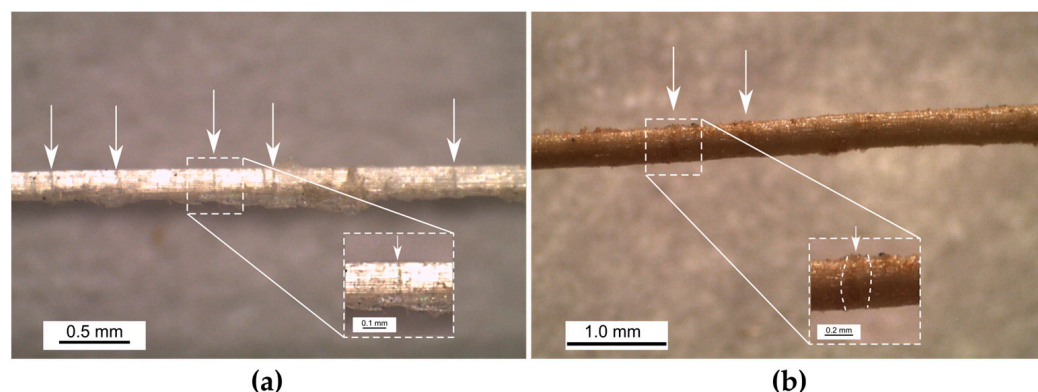
Figure 4. Light micrographs of micro-compressive defects in (**a**) banana and (**b**) coir raw fibers.

3.2. Fourier Transform Infrared Spectroscopy Analysis

Figure 5 shows the FTIR spectrums of banana and coir fibers with and without treatment. Both the untreated and treated fibers exhibited typical vibrational bands corresponding mainly to cellulose, hemicellulose, and lignin [44]. The aforementioned observation confirms the results of the composition analysis presented in Table 1, where it was noted that cellulose was the primary constituent of the fibers, followed by lignin and hemicelluloses. In BF/U, a broad and strong absorption band around 3330 cm^{-1} was observed, which corresponds to hydroxyl groups (OH) and can be attributed to the stretching of the O-H group in cellulose, hemicellulose, and lignin [45]. The stretching vibrations around 2840–2940 cm^{-1} can be associated with the C-H groups of cellulose and hemicellulose [46]. The absorption band in the range 1625–1660 cm^{-1} could be due to the stretching of carbonyl groups (C=O) in hemicellulose and possibly fatty acids from lignin [44]. A strong absorption band was observed at 1022 cm^{-1}, which was related to the stretching vibration of the C-O groups of cellulose, hemicellulose, and lignin [46,47]. After alkaline treatment, the absorption intensity in the band decreased at 3330 cm^{-1}, which is associated with the stretching of hydroxyl groups, indicating a possible cleavage of hydrogen bonds in the O-H groups in the hemicellulose of BF/T [46]. This observed effect could reduce the tendency of moisture absorption in the fibers and improve the interfacial bonding in the polymer matrices [48]. Moreover, a decrease in the band around 1610 cm^{-1} and the absence of the absorption band at 1321 cm^{-1} were observed, which could be related to the partial removal of lignin by the alkaline treatment [44,46]. These results indicate a decrease in hemicellulose and lignin content in the treated banana fibers. In coir fibers, a change in chemical composition after alkali treatment was also evident from the FTIR spectra. The increase in the absorption intensity of the band at about 3330 cm^{-1} can be attributed to the high accessibility of the O-H group after alkaline treatment, which can be associated with the removal of waxy substances on the fiber surface [49]. The increase in the peak at 1610 cm^{-1} in CF/T can be related to the removal of waxy substances and pectin [49]. The absorption peak at 1720 cm^{-1} in CF/U may be related to the vibration of the stretching of the acetyl and ester groups of hemicellulose, although it may also be due to the carboxyl groups (C=O) in lignin [12], while the peak observed at 1230 cm^{-1} is related to the stretching of the phenol group in lignin [12]. In CF/T, it is observed that the bands attributed to these components are not found, confirming their partial removal after the alkaline treatment. A peak around 2360 cm^{-1} was observed in the FTIR spectra, which does not belong to the functional groups present in the components of the lignocellulosic fibers and may be associated with impurities such as waxes and fats present on the surface [29,50]. However, the absorption intensity of the peak at 2360 cm^{-1} was lower after alkaline treatment, which could be related to the removal of impurities on the fiber surface [50].
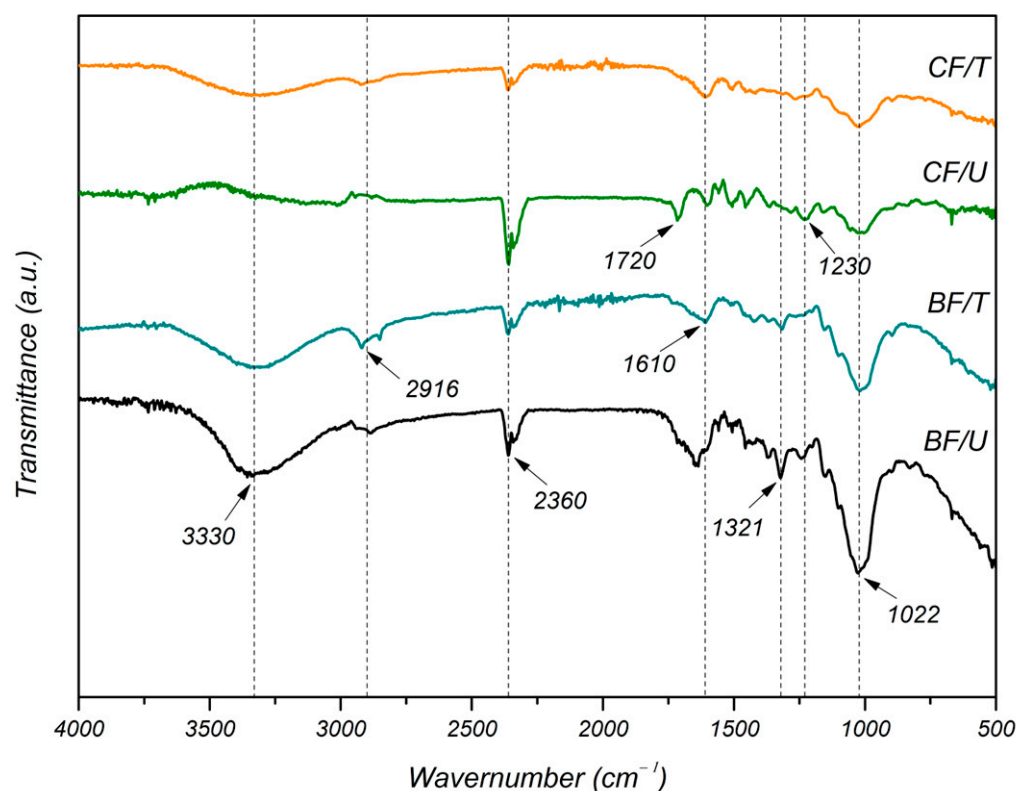
Figure 5. FTIR spectra of untreated and treated fibers.

3.3. Scanning Electron Microscopy

Figure 6 shows SEM images of the morphology of both the surface and cross-section of untreated banana and coir fibers. The structures of these fibers consist of several elementary fibers aligned in the longitudinal direction of the fiber (see Figure 6a,b). Banana fibers have an irregular surface covered with a layer of impurities, which may include hemicellulose and lignin compounds. Also, other non-cellulosic substances are present on the surface, such as pectin and waxes, which serve as natural binders and remain after extraction (Figure 6c) [12,29,51]. As may be observed in Figure 6d, Coir fibers generally have a smooth surface because a wax layer covers its surface structure [49,52]. Figure 6e,f show the cross-section of banana and coir fibers, aiming to understand their hierarchical structure. It can be observed from the images that the fiber bundles consist of several small cylindrical structures with a central cavity (lumen) extending along their cross-section. These structures are characteristic of natural fibers (elementary fibers) surrounded by a cementation region known as the middle lamella [12,41,49]. Each elementary fiber has a polygonal shape, which, is formed by the lumen and the cell wall. The cell wall consists of cellulose microfibrils agglomerated in a matrix of hemicellulose and lignin that extends along its entire length [7,8]. Therefore, the morphological characteristics associated with the hierarchical structures of the fibers can influence their mechanical properties [34].

The surface morphologies and cross-sections of coir and banana fibers after treatment are shown in the SEM images in Figure 7. BF/T showed an increase in surface roughness, which could be related to the removal of non-cellulosic components and surface impurities (Figure 7b) [53]. The aforementioned is important because it could facilitate the mechanical interlocking of the fiber in the polymer matrix, creating a possible physical interconnection between the two materials [54]. In addition, the reaction between the NaOH solution and the hydroxyl groups in the non-cellulosic constituents promotes the dissolution of hemicellulose, lignin, and some impurities, resulting in a smooth surface [55]. A marked thickening of the cell wall and collapse of the lumen were also seen in the cross-section of BF/Ts (Figure 7e). The latter can be attributed to a change in the cell wall caused by

the degradation of lignin and hemicellulose by the alkaline treatment [56,57]. As observed in BF/T, CF/T exhibited a rough surface with visible bulges and grooves, which can be attributed to the removal of waxes on the fiber surface (Figure 7d) [52]. The latter is of greater importance because the increased surface roughness of the treated coir fibers may affect the load transfer from the fiber to the matrix by mechanical interlocking [58]. After treatment, a partial deformation of the lumen size of the elementary fibers was observed (Figure 7f). This could be related to the morphological change in the coir fibers after alkaline treatment, resulting from the removal of the non-cellulosic substances around the lumen [59].
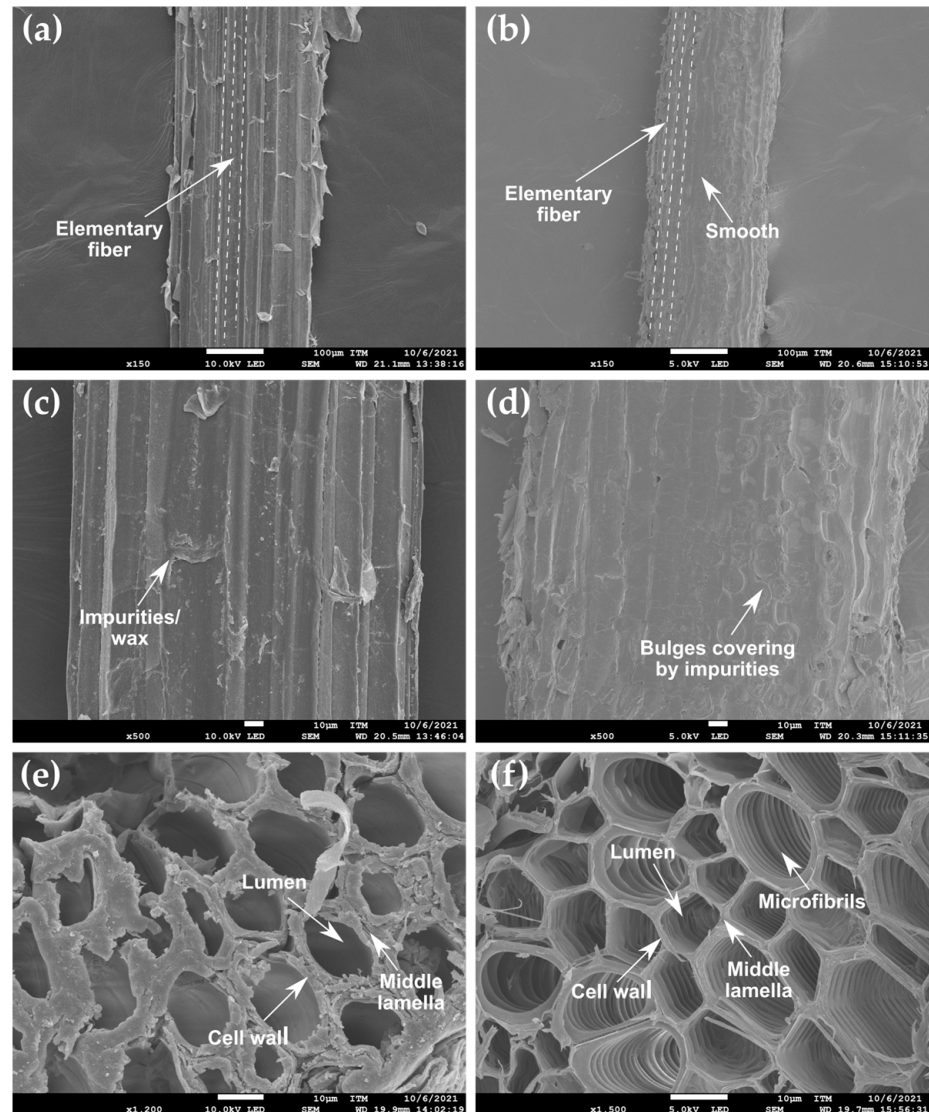
Figure 6. SEM images of the surface morphology of untreated fibers: (**a**) banana fiber (BF/U), (**b**) coir fiber (CF/U), (**c**) BF/U magnified to 500×, (**d**) CF/U magnified to 500×, and their cross-sections: (**e**) BF/U and (**f**) CF/U.
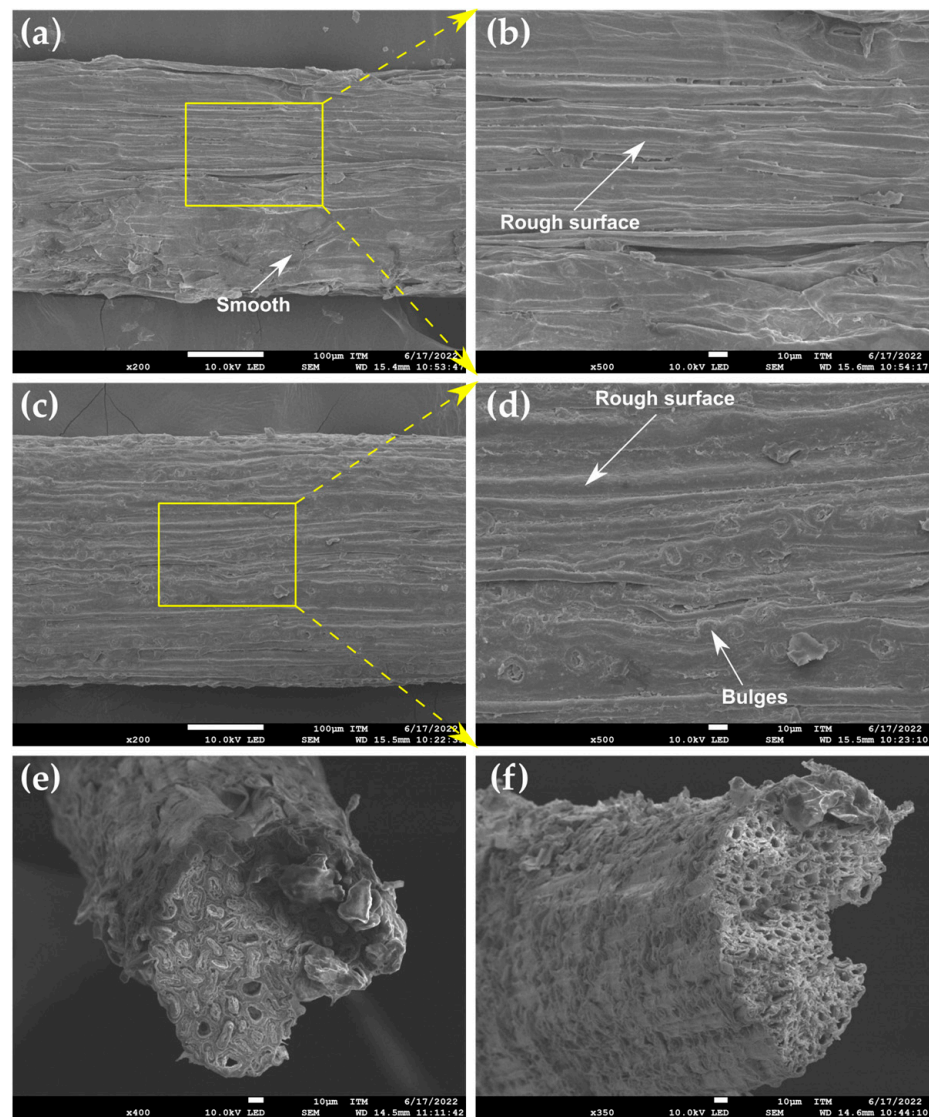
Figure 7. SEM images of the surface morphologies of treated fibers: (**a**) banana fiber (BF/T), (**b**) BF/T magnified to 500×, (**c**) coir fiber (CF/T), (**d**) CF/T magnified to 500×, and their cross-sections: (**e**) BF/T and (**f**) CF/T.

3.4. Thermogravimetric Results Analysis

The thermogravimetric analysis (TGA) and first derivative (DTG) curves of treated and untreated fibers are shown in Figure 8. The thermal degradation of the fibers shows phases that could be associated with moisture evaporation, removal of extractives, and decomposition of typical natural fiber constituents such as hemicellulose, cellulose, and lignin. A first phase of weight loss was observed in treated and untreated banana fibers in a temperature range from 25 to ~125 °C, which was attributed to the removal of moisture present on the fiber surface (Figure 8a) [60]. The DTG curve of BF/U in Figure 8b shows a peak at 200 °C with a weight loss of ~6%, which could be due to the removal of extractives such as waxes or fats and the decomposition of non-cellulosic components [61,62]. The absence of this peak in BF/T could be due to the removal of these non-cellulosic materials and surface impurities after the alkaline treatment. Figure 8b shows that the thermal degradation of BF/T started at a temperature of 200 °C, while that of BF/U started at about 250 °C, with maximum decomposition temperatures of 319 and 330 °C, respectively, which can be represented as the highest peak in the DTG curves. The treated banana fibers exhibited higher resistance to thermal degradation than untreated fibers due to the removal

of hemicellulose, lignin, and waxy substances and rapid weight loss, indicating higher thermal stability in BF/T due to alkaline treatment [62,63]. Figure 8c,d show the TGA and DTG curves of coir fibers with and without treatment, respectively. Differences in the thermal decomposition of the fibers are evident from the TGA curve. The TGA curves for CF/U show three phases of weight loss of 6.5, 19.7, and 41.7%, which were correlated with three distinct peaks at 44.7, 299, and 352 °C in the DTG curve, while the TGA curves of CT/F show two phases of weight loss of 4.90 and 53%. The TGA curves of CT/F show two phases of weight loss of 4.90 and 53%, which were correlated with two different peaks at 55.9 and 330 °C, respectively, in the DTG curve. The absence of the third phase in CF/T at 250 to 311 °C could be due to the removal of hemicellulose, lignin, and pectin from the coir fibers after alkaline treatment [59]. The results of thermogravimetric analysis, SEM, and FTIR analyses of treated and untreated fibers are consistent.
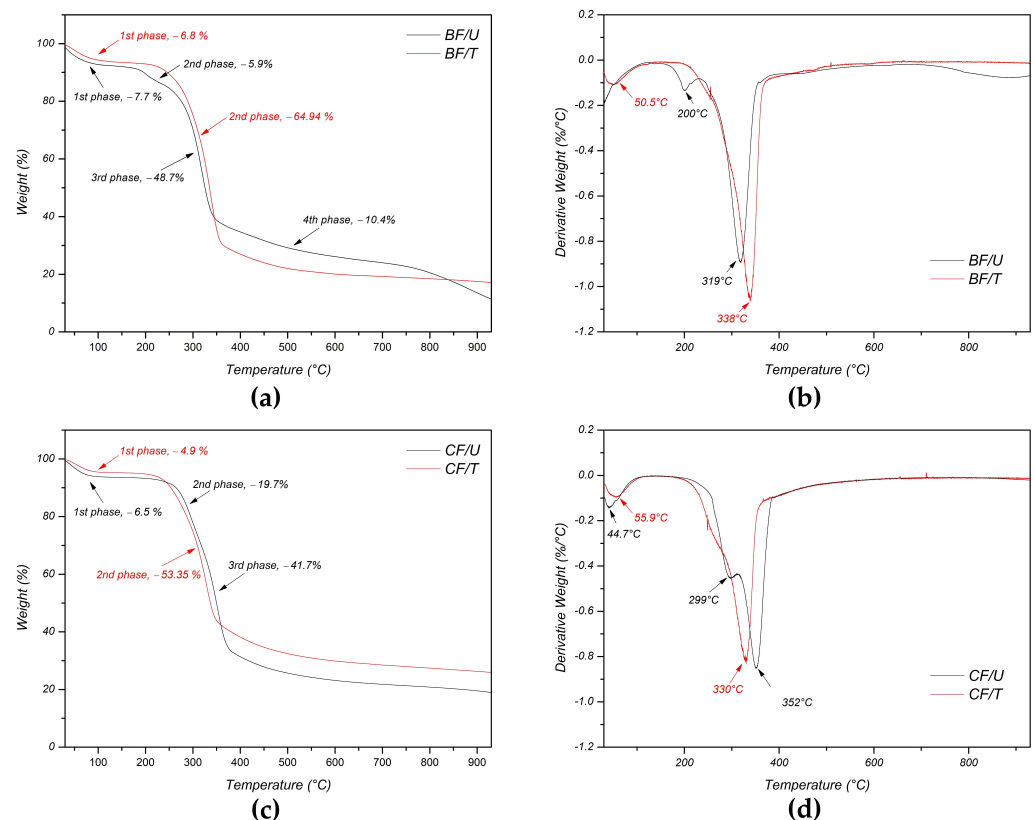
Figure 8. (**a**,**b**) TGA and DTG curves of untreated (black) and treated (red) banana fibers and (**c**,**d**) TGA and DTG curves of untreated (black) and treated (red) coir fibers.

3.5. Fiber–Matrix Adhesion Behavior

Table 4 shows the average interfacial shear strength (IFSS) values and percentage of broken fibers obtained from the pull-out tests of treated and untreated fibers with PLA and UPR matrices, while Figure 9 shows the load vs. displacement curves obtained in the pull-out tests for each system. To calculate the percentage of broken fibers in each specimen, the number of fibers broken during the pull-out test was divided by the total number of fibers tested [64]. During the pull-out test, it was observed that all BF/PLA/T and BF/UPR/T samples exhibited a percentage of 100% of broken fibers. Therefore, it was not possible to determine the IFSS value for these samples. In contrast, the BF/PLA and BF/UPR samples with untreated fibers had average IFSS values of 1.26 and 0.64 MPa, respectively, with corresponding percentages of 0% and 50% of broken fibers. Figure 9a,b show that samples BF/UPR/T and BF/PLA/T exhibit a sudden drop in the load vs. displacement curves, which could be related to fiber breakage during linear elastic deformation due to stress concentration at a specific point in the fiber [65]. However, it is believed the

sudden rupture of fibers can be influenced by the presence of micro-compressive defects or dislocations, as mentioned in Section 3.1. It is also suspected that the higher percentage of broken fibers in the treated samples is due to the influence of the alkaline treatment, which may increase the dislocations in the fibers and decrease their mechanical performance [66]. Moreover, treated banana fibers embedded in a UPR matrix achieved the highest force before breakage compared to fibers embedded in PLA. This is possibly due to the low viscosity of the UPR matrix compared to the PLA matrix during sample preparation, which allows better wetting of the fibers using UPR resin [43]. In the load vs. displacement curves for the BF/PLA/U and BF/UPR/U samples it is possible to observe a discontinuous drop, indicating the occurrence of frictional sliding while the fibers were being pulled out [67,68]. The abovementioned could be due to the low roughness of the untreated fiber surface, which leads to poor mechanical interlocking of the fiber with the matrix and weakening of the interfacial bonding between the fiber and matrix [69,70]. The observed behavior could explain the slight decrease in the percentage of broken fibers observed in the samples prepared with untreated fibers.

Table 4. Average interfacial shear strength (IFSS) values and percentages of broken fibers of pull-out specimens.

Specimen	IFSS (MPa)	%, Broke of Fiber	Specimen
BF/UPR/T	--	100	BF/UPR/T
BF/PLA/T	--	100	BF/PLA/T
BF/UPR/U	0.64	50	BF/UPR/U
BF/PLA/U	1.26 ($\pm$0.155)	0	BF/PLA/U
CF/UPR/T	1.01 ($\pm$0.356)	20	CF/UPR/T
CF/PLA/T	0.75 ($\pm$0.281)	50	CF/PLA/T
CF/UPR/U	0.92 ($\pm$0.261)	11	CF/UPR/U
CF/PLA/U	0.92 ($\pm$0.236)	0	CF/PLA/U
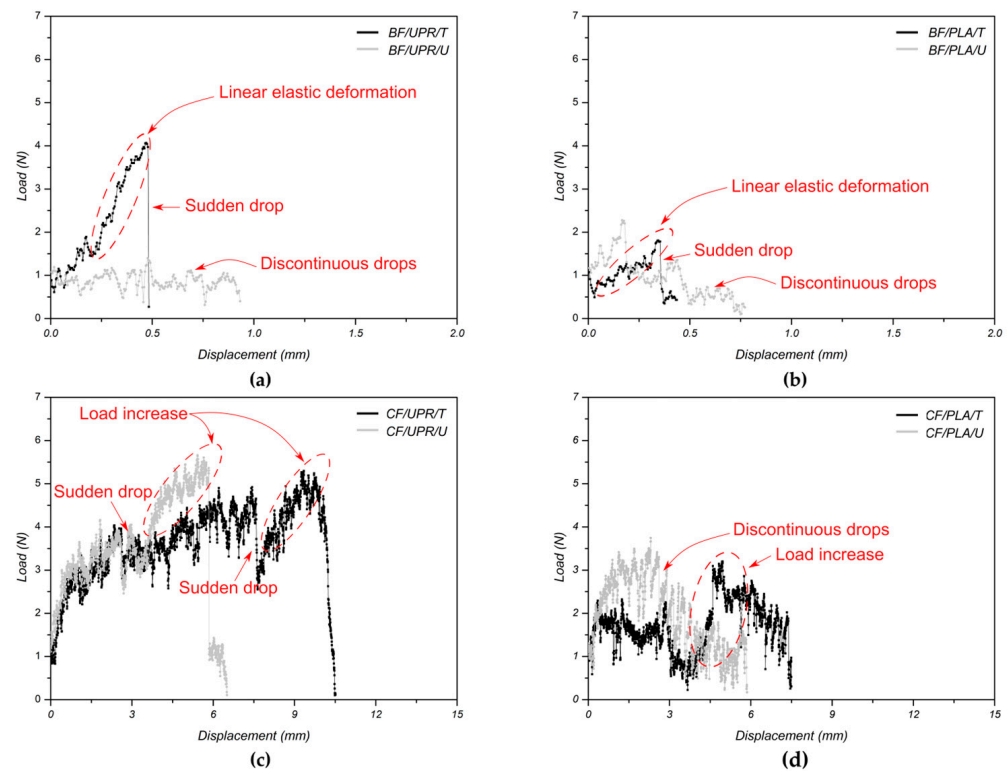
Figure 9. Load vs. displacement curves of systems: (**a**) BF/UPR, (**b**) BF/PLA, (**c**) CF/UPR, and (**d**) CF/PLA.

The average IFSS and percentage of broken fibers values for the coir fiber samples treated with PLA and UPR matrices were 0.75 and 1.01 MPa, 50% and 20%, respectively. While the untreated samples of CF had a similar IFSS average value of 0.92 MPa for both PLA and UPR matrices, their percentage of broken fibers was 0% and 11% for CF/PLA and CF/UPR, respectively. Among all tested coir fiber samples, the CF/UPR/T samples exhibited the highest average IFSS value, approximately 10% higher than that of the CF/UPR/U samples. However, the variability in the data suggests that there are no significant statistical differences between these IFSS values. The abovementioned observation is supported by Figure 9c, which shows a comparison of loading behavior in the pull-out test for both samples. Moreover, the CF/UPR curves display a discontinuous stage characterized by a brief decrease in loading, followed by a sudden drop, and then a slow increase during the loading process until the pulled-out fibers. The sudden drop in the pull-out curves could be attributed to the premature detachment of fibers in the matrix during the loading process [65]. However, the natural irregularities present in coir fibers (bulges and grooves) can create a mechanical interlocking effect. This can allow them to continue transferring the load even after the fiber–matrix bond breaks [71], resulting in a second stage of increasing load in the pull-out curves. Furthermore, it may be observed that the curve for the CF/UPR/T samples had a higher displacement than that of the CF/UPR/U samples. Alkaline treatment of the coir fiber surface led to the removal of non-cellulosic components and surface impurities, resulting in increased surface roughness. A rougher surface favors the formation of a potential physical interconnection between the fiber and the matrix [54]. Therefore, this may have facilitated better mechanical interlocking in the treated fibers [70,72]. On the other hand, higher discontinuities were observed in the pull-out curves of the CF/PLA/U samples compared to the samples prepared in the UPR matrix (See Figure 9d). This can be attributed to poor adhesion and wetting of the fibers in the PLA matrix, as already mentioned in the case of banana fibers. Observed behavior was attributed to the lack of penetration of PLA into the fiber surface structure after the matrix solidified as a function of the preparation method. The abovementioned together with the inherent brittleness of PLA could lead to early fiber detachment and a weaker interface in the tested samples [73]. In the case of CF/PLA/T samples (See Figure 9d), a sudden drop in the curve followed by a slight increase during loading was observed. This may be related to the effect of mechanical interlocking due to the increased roughness of the treated coir fibers. This could explain the slight decrease in the percentage of broken fibers observed in the samples prepared with untreated coir fibers.

4. Conclusions

In this study, the effects of alkaline treatment on the physicochemical, mechanical, and thermal properties of banana and coir fibers and their adhesion behavior when embedded in a PLA and UPR matrix were investigated. The ANOVA analysis of the mechanical properties of the studied fibers revealed that only the surface treatment significantly affected the Young's modulus. This effect is attributed to the structural changes that occur when non-cellulosic components are removed during mercerization treatment. In contrast, the tensile strength and elongation at break were not influenced by the surface treatment, as indicated by a *p*-value greater than 0.05. In addition, FTIR analysis showed that the non-cellulosic components were removed after alkaline treatment, while SEM images showed an increase in fiber surface roughness associated with the removal of surface impurities. This facilitated the mechanical interlocking of the treated fibers with PLA and UPR. Thermogravimetric analysis showed that the treated banana fibers exhibited higher resistance to thermal degradation and thermal stability. This was attributed to the removal of hemicellulose, lignin, and waxy substances from the fibers. A change in thermal degradation was observed in the treated coir fibers, possibly related to the removal of hemicellulose, lignin, and pectin from the fibers. On the other hand, the untreated samples had average IFSS values of 1.26 and 0.64 MPa, with corresponding percentages of 0% and 50% of broken fibers, respectively. This was attributed to the low roughness of the untreated

fiber surface, which resulted in poor mechanical interlocking with the matrix and weak interfacial bonding between the fiber and matrix. In contrast, the treated banana fibers produced in PLA and UPR matrices had a percentage of broken fibers of 100%, so it was not possible to determine the IFSS value. This fact was attributed to the increase in micro-compressive defects or dislocations along the fibers because of alkali treatment, which may reduce their mechanical performance. The treated coir fibers embedded in a UPR matrix showed better adhesion behavior than the samples prepared in a PLA matrix, with the CF/UPR/T samples having the highest average IFSS value, which was about 10% higher than that of the CF/UPR/U. This fact was attributed to the effect of alkaline treatment on the fiber surface, which removed non-cellulosic components and impurities, resulting in increased surface roughness. This, in turn, facilitated better mechanical interlocking between the fiber and the matrix, resulting in improved interfacial adhesion. In addition, the CF/PLA samples exhibited poorer adhesion behavior than the CF/UPR samples, which can be attributed to the poor adhesion and wetting of the fibers with the PLA matrix.

Author Contributions: Conceptualization, O.R.-R. and J.U.-S.; formal analysis, I.B.-F. and O.R.-R.; investigation, I.B.-F.; writing—review and editing, O.R.-R. and J.U.-S.; supervision, J.U.-S. All authors have read and agreed to the published version of the manuscript.

Institutional Review Board Statement: Not applicable.

Data Availability Statement: The data presented in this study are available upon request from the corresponding author. For data protection reasons, the data are not publicly accessible.

Conflicts of Interest: The authors declare no conflicts of interest.

References

1. Gurunathan, T.; Mohanty, S.; Nayak, S.K. A Review of the Recent Developments in Biocomposites Based on Natural Fibres and Their Application Perspectives. *Compos. Part. A Appl. Sci. Manuf.* **2015**, *77*, 1–25. [CrossRef]
2. Saindane, U.V.; Soni, S.; Menghani, J.V. Recent Research Status on Synthesis and Characterization of Natural Fibers Reinforced Polymer Composites and Modern Friction Materials—An Overview. *Proc. Mater. Today Proc.* **2019**, *26*, 1616–1620. [CrossRef]
3. Zarna, C.; Opedal, M.T.; Echtermeyer, A.T.; Chinga-Carrasco, G. Reinforcement Ability of Lignocellulosic Components in Biocomposites and Their 3D Printed Applications—A Review. *Compos. Part C Open Access* **2021**, *6*, 100171. [CrossRef]
4. Patel, B.Y.; Patel, H.K. Retting of Banana Pseudostem Fibre Using Bacillus Strains to Get Excellent Mechanical Properties as Biomaterial in Textile & Fiber Industry. *Heliyon* **2022**, *8*, e10652. [CrossRef] [PubMed]
5. Yang, J.; Li, N.; Wang, C.; Chang, T.; Jiang, H. Ultrasound-Homogenization-Assisted Extraction of Polyphenols from Coconut Mesocarp: Optimization Study. *Ultrason. Sonochem.* **2021**, *78*, 105739. [CrossRef] [PubMed]
6. Yaashikaa, P.R.; Senthil Kumar, P.; Varjani, S. Valorization of Agro-Industrial Wastes for Biorefinery Process and Circular Bioeconomy: A Critical Review. *Bioresour. Technol.* **2022**, *343*, 126126. [CrossRef] [PubMed]
7. Oushabi, A. The Pull-out Behavior of Chemically Treated Lignocellulosic Fibers/Polymeric Matrix Interface (LF/PM): A Review. *Compos. B Eng.* **2019**, *174*, 107059. [CrossRef]
8. Lee, C.H.; Khalina, A.; Lee, S.H. Importance of Interfacial Adhesion Condition on Characterization of Plant-Fiber-Reinforced Polymer Composites: A Review. *Polymers* **2021**, *13*, 438. [CrossRef]
9. Akintayo, C.O.; Azeez, M.A.; Beuerman, S.; Akintayo, E.T. Spectroscopic, Mechanical, and Thermal Characterization of Native and Modified Nigerian Coir Fibers. *J. Nat. Fibers* **2016**, *13*, 520–531. [CrossRef]
10. Sathish, S.; Karthi, N.; Prabhu, L.; Gokulkumar, S.; Balaji, D.; Vigneshkumar, N.; Ajeem Farhan, T.S.; Akilkumar, A.; Dinesh, V.P. A Review of Natural Fiber Composites: Extraction Methods, Chemical Treatments and Applications. *Mater. Today Proc.* **2021**, *45*, 8017–8023. [CrossRef]
11. Žiganova, M.; Ābele, A.; Iesalniece, Z.; Meri, R.M. Mercerization of Agricultural Waste: Sweet Clover, Buckwheat, and Rapeseed Straws. *Fibers* **2022**, *10*, 83. [CrossRef]

12. Jaramillo-Quiceno, N.; Vélez R, J.M.; Cadena Ch, E.M.; Restrepo-Osorio, A.; Santa, J.F. Improvement of Mechanical Properties of Pineapple Leaf Fibers by Mercerization Process. *Fibers Polym.* **2018**, *19*, 2604–2611. [CrossRef]

13. Ernest, E.M.; Peter, A.C. Application of Selected Chemical Modification Agents on Banana Fibre for Enhanced Composite Production. *Clean. Mater.* **2022**, *5*, 100131. [CrossRef]

14. Sawpan, M.A.; Pickering, K.L.; Fernyhough, A. Effect of Various Chemical Treatments on the Fibre Structure and Tensile Properties of Industrial Hemp Fibres. *Compos. Part A Appl. Sci. Manuf.* **2011**, *42*, 888–895. [CrossRef]

15. Da Luz, F.S.; Ramos, F.J.H.T.V.; Nascimento, L.F.C.; Figueiredo, A.B.H.D.S.; Monteiro, S.N. Critical Length and Interfacial Strength of PALF and Coir Fiber Incorporated in Epoxy Resin Matrix. *J. Mater. Res. Technol.* **2018**, *7*, 528–534. [CrossRef]

16. Mokaloba, N.; Batane, R. The Effects of Mercerization and Acetylation Treatments on the Properties of Sisal Fiber and Its Interfacial Adhesion Characteristics on Polypropylene. *Int. J. Eng. Sci. Technol.* **2014**, *6*, 83. [CrossRef]

17. Gayathri, N.; Shanmuganathan, V.K.; Joyson, A.; Aakash, M.; Godwin Joseph, A. Mechanical Properties Investigation on Natural Fiber Reinforced Epoxy Polymer Composite. *Mater. Today Proc.* **2023**, *72*, 2574–2580. [CrossRef]

18. Pitchayya Pillai, G.; Manimaran, P.; Vignesh, V. Physico-Chemical and Mechanical Properties of Alkali-Treated Red Banana Peduncle Fiber. *J. Nat. Fibers* **2021**, *18*, 2102–2111. [CrossRef]

19. Javanshour, F.; Prapavesis, A.; Pournoori, N.; Soares, G.C.; Orell, O.; Pärnänen, T.; Kanerva, M.; Van Vuure, A.W.; Sarlin, E. Impact and Fatigue Tolerant Natural Fibre Reinforced Thermoplastic Composites by Using Non-Dry Fibres. *Compos. Part A Appl. Sci. Manuf.* **2022**, *161*, 107110. [CrossRef]

20. Jänicke, G.; Vintache, A.; Smaniotto, B.; Fau, A.; Farina, I.; Fraternali, F.; Hild, F. Debonding Analysis via Digital Volume Correlation during In-Situ Pull-out Tests on Fractal Fibers. *Compos. Part C Open Access* **2022**, *9*, 100302. [CrossRef]

21. Garcia-Diaz, Y.; Torres-Ortega, R.; Tovar, C.T.; Quiñones-Bolaños, E.; Saba, M. Characterization of Pull-out Behavior in the Fiber–Mortar Interface with Superficial Treatments. *Constr. Build. Mater.* **2021**, *303*, 124474. [CrossRef]

22. Huang, S.; Fu, Q.; Yan, L.; Kasal, B. Characterization of Interfacial Properties between Fibre and Polymer Matrix in Composite Materials—A Critical Review. *J. Mater. Res. Technol.* **2021**, *13*, 1441–1484. [CrossRef]

23. Zhang, Z.; Li, Y.; Fu, K.; Li, Q. Determination of Interfacial Properties of Cellulose Nanocrystal-Modified Sisal Fibre in Epoxy by Cyclic Single-Fibre Pull-Out. *Compos. Sci. Technol.* **2020**, *193*, 108142. [CrossRef]

24. Merlini, C.; Soldi, V.; Barra, G.M.O. Influence of Fiber Surface Treatment and Length on Physico-Chemical Properties of Short Random Banana Fiber-Reinforced Castor Oil Polyurethane Composites. *Polym. Test.* **2011**, *30*, 833–840. [CrossRef]

25. Nam, T.H.; Ogihara, S.; Tung, N.H.; Kobayashi, S. Effect of Alkali Treatment on Interfacial and Mechanical Properties of Coir Fiber Reinforced Poly(Butylene Succinate) Biodegradable Composites. *Compos. B Eng.* **2011**, *42*, 1648–1656. [CrossRef]

26. Madyira, D.M.; Kaymakci, A. Mechanical Characterization of Coir Epoxy Composites and Effect of Processing Methods on Mechanical Properties. In Proceedings of the International Conference on Competitive Manufacturing COMA 16, Stellenbosch, South Africa, 27–29 January 2016. Available online: https://hdl.handle.net/10210/123894 (accessed on 21 March 2023).

27. Rivero-Romero, O.; Barrera-Fajardo, I.; Unfried-Silgado, J. Effects of Printing Parameters on Fiber Eccentricity and Porosity Level in a Thermoplastic Matrix Composite Reinforced with Continuous Banana Fiber Fabricated by FFF with in Situ Impregnation. *Int. J. Adv. Manuf. Technol.* **2023**, *125*, 1893–1901. [CrossRef]

28. Buelvas, Y.; Díaz, L. Caracterización de Fibras del Mesocarpio del coco como Potencial Refuerzo para la Elaboración de Materiales Compuestos. Undergraduate Thesis, Universidad de Córdoba, Córdoba, Colombia, 2023. Available online: https://repositorio.unicordoba.edu.co/handle/ucordoba/7177 (accessed on 4 April 2023).

29. Montoya, J.; Negrete, J. Caracterización de la Fibra del Pseudotallo del Plátano como Potencial Refuerzo para la Elaboración de Materiales Compuestos. Undergraduate Thesis, Universidad de Córdoba, Córdoba, Colombia, 2023. Available online: https://repositorio.unicordoba.edu.co/handle/ucordoba/7173 (accessed on 3 April 2023).

30. Hall, M.B.; Mertens, D.R. Comparison of Alternative Neutral Detergent Fiber Methods to the AOAC Definitive Method. *J. Dairy Sci.* **2023**, *106*, 5364–5378. [CrossRef]

31. Ossa Henao, D.M.; Chica Arrieta, E.L.; Colorado Granda, A.F.; Amell Arrieta, A.A.; Unfried-Silgado, J. Characterization of Bovine Ruminal Content Focusing on Energetic Potential Use and Valorization Opportunities. *Heliyon* **2023**, *9*, e13408. [CrossRef]

32. *ASTM C1557-20*; Standard Test Method for Tensile Strength and Young's Modulus of Fibers, Book of Standards Volume: 15.01, Developed by Subcommittee: C28.07. ASTM International: West Conshohocken, PA, USA, 2020; p. 11.

33. Mathura, N.; Cree, D. Characterization and Mechanical Property of Trinidad Coir Fibers. *J. Appl. Polym. Sci.* **2016**, *133*, 1–9. [CrossRef]

34. Valášek, P.; Müller, M.; Šleger, V.; Kolář, V.; Hromasová, M.; D'amato, R.; Ruggiero, A. Influence of Alkali Treatment on the Microstructure and Mechanical Properties of Coir and Abaca Fibers. *Materials* **2021**, *14*, 2636. [CrossRef]

35. Amiandamhen, S.O.; Meincken, M.; Tyhoda, L. Natural Fibre Modification and Its Influence on Fibre-Matrix Interfacial Properties in Biocomposite Materials. *Fibers Polym.* **2020**, *21*, 677–689. [CrossRef]

36. Gleadall, A. FullControl GCode Designer: Open-Source Software for Unconstrained Design in Additive Manufacturing. *Addit. Manuf.* **2021**, *46*, 102109. [CrossRef]

37. Hestiawan, H.; Jamasri; Kusmono. Effect of Chemical Treatments on Tensile Properties and Interfacial Shear Strength of Unsaturated Polyester/Fan Palm Fibers. *J. Nat. Fibers* **2018**, *15*, 762–775. [CrossRef]

38. Oushabi, A.; Sair, S.; Oudrhiri, H.F.; Abboud, Y.; Tanane, O.; El Bouari, A. The effect of alkali treatment on mechanical, morphological and thermal properties of date palm fibers (DPFs): Study of the interface of DPF–Polyurethane composite. *S. Afr. J. Chem. Eng.* **2017**, *23*, 116–123. [CrossRef]

39. Chokshi, S.; Parmar, V.; Gohil, P.; Chaudhary, V. Chemical Composition and Mechanical Properties of Natural Fibers. *J. Nat. Fibers* **2022**, *19*, 3942–3953. [CrossRef]

40. Rajeshkumar, G.; Arvindh Seshadri, S.; Devnani, G.L.; Sanjay, M.R.; Siengchin, S.; Prakash Maran, J.; Al-Dhabi, N.A.; Karuppiah, P.; Mariadhas, V.A.; Sivarajasekar, N.; et al. Environment Friendly, Renewable and Sustainable Poly Lactic Acid (PLA) Based Natural Fiber Reinforced Composites—A Comprehensive Review. *J. Clean. Prod.* **2021**, *310*, 127483. [CrossRef]

41. Valášek, P.; D'Amato, R.; Müller, M.; Ruggiero, A. Mechanical Properties and Abrasive Wear of White/Brown Coir Epoxy Composites. *Compos. B Eng.* **2018**, *146*, 88–97. [CrossRef]

42. Hernandez-Estrada, A.; Gusovius, H.J.; Müssig, J.; Hughes, M. Assessing the Susceptibility of Hemp Fibre to the Formation of Dislocations during Processing. *Ind. Crops Prod.* **2016**, *85*, 382–388. [CrossRef]

43. Sawpan, M.A.; Pickering, K.L.; Fernyhough, A. Effect of Fibre Treatments on Interfacial Shear Strength of Hemp Fibre Reinforced Polylactide and Unsaturated Polyester Composites. *Compos. Part A Appl. Sci. Manuf.* **2011**, *42*, 1189–1196. [CrossRef]

44. Twebaze, C.; Zhang, M.; Zhuang, X.; Kimani, M.; Zheng, G.; Wang, Z. Banana Fiber Degumming by Alkali Treatment and Ultrasonic Methods. *J. Nat. Fibers* **2022**, *19*, 12911–12923. [CrossRef]

45. Kannan, G.; Thangaraju, R. Evaluation of Tensile, Flexural and Thermal Characteristics on Agro-Waste Based Polymer Composites Reinforced with Banana Fiber/Coconut Shell Filler. *J. Nat. Fibers* **2023**, *20*, 2154630. [CrossRef]

46. Oyewo, A.T.; Oluwole, O.O.; Ajide, O.O.; Omoniyi, T.E.; Akhter, P.; Hamayun, M.H.; Kang, B.S.; Park, Y.K.; Hussain, M. Physico-Chemical, Thermal and Micro-Structural Characterization of Four Common Banana Pseudo-Stem Fiber Cultivars in Nigeria. *J. Nat. Fibers* **2023**, *20*, 2167031. [CrossRef]

47. Badanayak, P.; Jose, S.; Bose, G. Banana Pseudostem Fiber: A Critical Review on Fiber Extraction, Characterization, and Surface Modification. *J. Nat. Fibers* **2023**, *20*, 2168821. [CrossRef]

48. Gupta, U.S.; Dhamarikar, M.; Dharkar, A.; Chaturvedi, S.; Tiwari, S.; Namdeo, R. Surface Modification of Banana Fiber: A Review. *Proc. Mater. Today Proc.* **2020**, *43*, 904–915. [CrossRef]

49. Mittal, M.; Chaudhary, R. Experimental Study on the Water Absorption and Surface Characteristics of Alkali Treated Pineapple Leaf Fibre and Coconut Husk fibre. *Int. J. Appl. Eng. Res.* **2018**, *13*, 12237–12243.

50. Soraisham, L.D.; Gogoi, N.; Mishra, L.; Basu, G. Extraction and Evaluation of Properties of Indian Banana Fibre (*Musa domestica* Var. Balbisiana, BB Group) and Its Processing with Ramie. *J. Nat. Fibers* **2022**, *19*, 5839–5850. [CrossRef]

51. Oladele, I.O.; Michael, O.S.; Adediran, A.A.; Balogun, O.P.; Ajagbe, F.O. Acetylation Treatment for the Batch Processing of Natural Fibers: Effects on Constituents, Tensile Properties and Surface Morphology of Selected Plant Stem Fibers. *Fibers* **2020**, *8*, 73. [CrossRef]

52. dos Santos, J.C.; Siqueira, R.L.; Vieira, L.M.G.; Freire, R.T.S.; Mano, V.; Panzera, T.H. Effects of Sodium Carbonate on the Performance of Epoxy and Polyester Coir-Reinforced Composites. *Polym. Test.* **2018**, *67*, 533–544. [CrossRef]

53. Senthamaraikannan, P.; Kathiresan, M. Characterization of Raw and Alkali Treated New Natural Cellulosic Fiber from *Coccinia grandis*.L. *Carbohydr. Polym.* **2018**, *186*, 332–343. [CrossRef]

54. Setswalo, K.; Molaletsa, N.; Oladijo, O.P.; Akinlabi, E.T.; Rangappa, S.M.; Siengchin, S. The Influence of Fiber Processing and Alkaline Treatment on the Properties of Natural Fiber-Reinforced Composites: A Review. *Appl. Sci. Eng. Prog.* **2021**, *14*, 632–650. [CrossRef]

55. Cadena Ch, E.M.; Vélez R, J.M.; Santa, J.F.; Otálvaro, G.V. Natural Fibers from Plantain Pseudostem (*Musa paradisiaca*) for Use in Fiber-Reinforced Composites. *J. Nat. Fibers* **2017**, *14*, 678–690. [CrossRef]

56. Ntimugura, F.; Wilson, K.; Vinai, R.; Walker, P. Effect of Alkali-Silica Treatments of Miscanthus Fibres on Chemical and Micro-Morphological Modifications. *Clean. Mater.* **2023**, *8*, 100182. [CrossRef]

57. Cai, M.; Takagi, H.; Nakagaito, A.N.; Katoh, M.; Ueki, T.; Waterhouse, G.I.N.; Li, Y. Influence of Alkali Treatment on Internal Microstructure and Tensile Properties of Abaca Fibers. *Ind. Crops Prod.* **2015**, *65*, 27–35. [CrossRef]

58. de Farias, J.G.G.; Cavalcante, R.C.; Canabarro, B.R.; Viana, H.M.; Scholz, S.; Simão, R.A. Surface Lignin Removal on Coir Fibers by Plasma Treatment for Improved Adhesion in Thermoplastic Starch Composites. *Carbohydr. Polym.* **2017**, *165*, 429–436. [CrossRef] [PubMed]

59. Ru, S.; Zhao, C.; Yang, S. Multi-Objective Optimization and Analysis of Mechanical Properties of Coir Fiber from Coconut Forest Waste. *Forests* **2022**, *13*, 33. [CrossRef]

60. Lai, T.S.M.; Jayamani, E.; Soon, K.H. Comparative Study on Thermogravimetric Analysis of Banana Fibers Treated with Chemicals. *Mater. Today Proc.* **2022**, *78*, 458–461. [CrossRef]

61. Komal, U.K.; Verma, V.; Aswani, T.; Verma, N.; Singh, I. Effect of Chemical Treatment on Mechanical Behavior of Banana Fiber Reinforced Polymer Composites. *Mater. Today Proc.* **2018**, *5*, 16983–16989. [CrossRef]

62. Hossain, M.K.; Karim, M.R.; Chowdhury, M.R.; Imam, M.A.; Hosur, M.; Jeelani, S.; Farag, R. Comparative Mechanical and Thermal Study of Chemically Treated and Untreated Single Sugarcane Fiber Bundle. *Ind. Crops Prod.* **2014**, *58*, 78–90. [CrossRef]

63. Maharana, S.M.; Pandit, M.K.; Pradhan, A.K. Effect of Chemical Treatment and Fumed Silica Coating on Tensile and Thermogravimetric Properties of Jute Yarn. *Proc. Mater. Today Proc.* **2019**, *27*, 2693–2698. [CrossRef]

64.   Boshoff, W.P.; Mechtcherine, V.; van Zijl, G.P.A.G. Characterising the Time-Dependant Behaviour on the Single Fibre Level of SHCC: Part 2: The Rate Effects on Fibre Pull-out Tests. *Cem. Concr. Res.* **2009**, *39*, 787–797. [CrossRef]

65.   Oliveira, M.S.; Pereira, A.C.; da Costa Garcia Filho, F.; da Cruz Demosthenes, L.C.; Monteiro, S.N. Performance of Epoxy Matrix Reinforced with Fique Fibers in Pullout Tests. In *Characterization of Minerals, Metals, and Materials 2019*; Li, B., Li, J., Ikhmayies, S., Zhang, M., Kalay, Y.E., Carpenter, J.S., Hwang, J.Y., Monteiro, S.N., Bai, C., Escobedo-Diaz, J.P., et al., Eds.; Minerals, Metals and Materials Series; Springer International Publishing: Berlin/Heidelberg, Germany, 2019; pp. 729–734.

66.   Richely, E.; Bourmaud, A.; Placet, V.; Guessasma, S.; Beaugrand, J. A Critical Review of the Ultrastructure, Mechanics and Modelling of Flax Fibres and Their Defects. *Prog. Mater. Sci.* **2022**, *124*, 100851. [CrossRef]

67.   Naik, D.L.; Sharma, A.; Chada, R.R.; Kiran, R.; Sirotiak, T. Modified Pullout Test for Indirect Characterization of Natural Fiber and Cementitious Matrix Interface Properties. *Constr. Build. Mater.* **2019**, *208*, 381–393. [CrossRef]

68.   Ferrara, G.; Pepe, M.; Martinelli, E.; Filho, R.D.T. Influence of an Impregnation Treatment on the Morphology and Mechanical Behaviour of Flax Yarns Embedded in Hydraulic Lime Mortar. *Fibers* **2019**, *7*, 30. [CrossRef]

69.   Nirmal, U.; Singh, N.; Hashim, J.; Lau, S.T.W.; Jamil, N. On the Effect of Different Polymer Matrix and Fibre Treatment on Single Fibre Pullout Test Using Betelnut Fibres. *Mater. Des.* **2011**, *32*, 2717–2726. [CrossRef]

70.   Huerta-Cardoso, O.; Durazo-Cardenas, I.; Marchante-Rodriguez, V.; Longhurst, P.; Coulon, F.; Encinas-Oropesa, A. Up-Cycling of Agave Tequilana Bagasse-Fibres: A Study on the Effect of Fibre-Surface Treatments on Interfacial Bonding and Mechanical Properties. *Results Mater.* **2020**, *8*, 100158. [CrossRef]

71.   Wang, B.; Yan, L.; Kasal, B. A Review of Coir Fibre and Coir Fibre Reinforced Cement-Based Composite Materials (2000–2021). *J. Clean. Prod.* **2022**, *338*, 130676. [CrossRef]

72.   Orue, A.; Jauregi, A.; Peña-Rodriguez, C.; Labidi, J.; Eceiza, A.; Arbelaiz, A. The Effect of Surface Modifications on Sisal Fiber Properties and Sisal/Poly (Lactic Acid) Interface Adhesion. *Compos. B Eng.* **2015**, *73*, 132–138. [CrossRef]

73.   Viel, Q.; Esposito, A.; Saiter, J.M.; Santulli, C.; Turner, J.A. Interfacial Characterization by Pull-out Test of Bamboo Fibers Embedded in Poly(Lactic Acid). *Fibers* **2018**, *6*, 7. [CrossRef]